Combustion and Flame 157 (2010) 2267–2276

Contents lists available at ScienceDirect

Combustion and Flame

journal homepage: www.elsevier.com/locate/combustflame

Effects of radiation and compression on propagating spherical flames of methane/air mixtures near the lean flammability limit

Zheng Chen *

State Key Laboratory for Turbulence and Complex Systems, Department of Mechanics and Aerospace Engineering, College of Engineering, Peking University, Beijing 100871, China

ARTICLE INFO

Article history:
Received 25 March 2010
Received in revised form 18 May 2010
Accepted 8 July 2010
Available online 3 August 2010

Keywords:
Laminar flame speed
Markstein length
Propagating spherical flame
Radiation
Compression

ABSTRACT

Large discrepancies between the laminar flame speeds and Markstein lengths measured in experiments and those predicted by simulations for ultra-lean methane/air mixtures bring a great concern for kinetic mechanism validation. In order to quantitatively explain these discrepancies, a computational study is performed for propagating spherical flames of lean methane/air mixtures in different spherical chambers using different radiation models. The emphasis is focused on the effects of radiation and compression. It is found that the spherical flame propagation speed is greatly reduced by the coupling between thermal effect (change of flame temperature or unburned gas temperature) and flow effect (inward flow of burned gas) induced by radiation and/or compression. As a result, for methane/air mixtures near the lean flammability limit, the radiation and compression cause large amounts of under-prediction of the laminar flame speeds and Markstein lengths extracted from propagating spherical flames. Since radiation and compression both exist in the experiments on ultra-lean methane/air mixtures reported in the literature, the measured laminar flame speeds and Markstein lengths are much lower than results from simulation and thus cannot be used for kinetic mechanism validation.

1. Introduction

The laminar flame speed and Markstein length are two fundamental parameters of a combustible mixture [1,2]. Their accurate determination is extremely important for validating chemical kinetic mechanisms [3] and for modeling turbulent premixed combustion within the laminar flamelet regime [4]. Therefore, in the last 50 years, substantial attention has been given to the determination of the laminar flame speed and Markstein length and various experimental approaches have been developed to measure these two parameters [5,6].

The most common approaches for measuring the laminar flame speed and Markstein length are the counterflow flame method [7,8] and the propagating spherical flame method [9–26]. Recently, Davis and coworkers [27,28] investigated the counterflow flames and found that the stretch rate measured at the position of local minimum flow velocity (or maximum velocity gradient) is not an accurate indicator of the stretch exerted on the flame. Therefore, it is difficult to accurately determine the Markstein length using the counterflow flame method [27,28]. Moreover, because of the Reynolds number limit, it is difficult to use the counterflow flame method to measure the laminar flame speed at high pressures [15]. Consequently, due to its simple flame configuration and well-defined flame stretch rate at normal and high pressures, the propagating spherical flame method is currently the most favorable method for measuring the laminar flame speed and Markstein length [9–26].

In the propagating spherical flame method, a quiescent homogeneous combustible mixture in a closed chamber is centrally ignited by an electrical spark which results in an outwardly propagating spherical flame [9–26]. The stretched flame speed and stretch rate are calculated from the flame front history, $R_f = R_f(t)$, which is recorded by schlieren or shadow photography. The unstretched laminar flame speed and Markstein length are then obtained from the linear extrapolation between the stretched flame speed and stretch rate. Recently, a great deal of effort has been devoted to obtaining accurate laminar flame speed and Markstein length from propagating spherical flames. For example, Bradley et al. [12] studied the effects of ignition and different isotherms on the spherical flame propagation speed; Qiao et al. [20] designed a short-drop free-fall laboratory facility that provides low gravity conditions (10^{-2} g) so that the effects of buoyancy can be minimized; Chen et al. [23] showed that the flame speed reverse phenomenon greatly narrows the experimental data range valid for flame speed extrapolation; Burke et al. [24] demonstrated that the flow field deviation due to non-spherical chambers can reduce the accuracy of flame speed measurements.

However, discrepancies among the laminar flame speeds and Markstein lengths measured by different researchers for the same

* Fax: +86 10 6275 7532.
E-mail address: cz@pku.edu.cn

0010-2180/$ - see front matter © 2010 The Combustion Institute. Published by Elsevier Inc. All rights reserved.
doi:10.1016/j.combustflame.2010.07.010

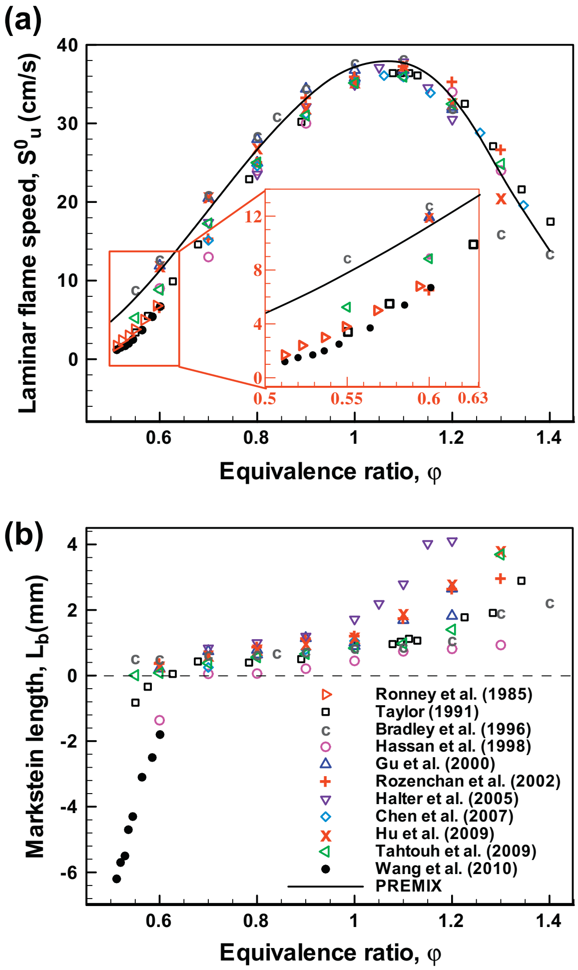

Fig. 1. (a) Laminar flame speed and (b) Markstein length relative to the burned gas for methane/air mixtures at atmospheric pressure and room temperature (symbols: results extracted from outwardly propagating spherical flames; line: results from simulation of adiabatic propagating planar flames).

fuel are still appearing in the literature [29,30] and become a great concern for kinetic mechanism validation. Figure 1 shows the measured laminar flame speeds, S_u^0, and the Markstein lengths relative to the burned gas, L_b, for the simplest hydrocarbon fuel, methane. Except for the laminar flame speed calculated by PREMIX (solid line) [31], all the experimental results (symbols) were measured using the propagating spherical flame method [10,14,16–18,21,22,25,26,32]. For near-stoichiometric and rich CH_4/air mixtures ($\varphi \geqslant 0.8$), relatively small discrepancies are shown to exist among the measured laminar flame speeds; unlike the laminar flame speeds, Fig. 1b shows that there are very large discrepancies for the Markstein lengths measured by different researchers and the relative difference can even be larger than 300% for $\varphi > 1.1$. For CH_4/air mixtures near the lean flammability limit ($\varphi \leqslant 0.65$), Fig. 1 shows that there are huge discrepancies among S_u^0 and L_b measured by different researchers and/or predicted from simulation. According to Ronney and Wachman [32], the buoyancy strongly affects the spherical flame propagation in normal-gravity experiments when S_u^0 is below 15 cm/s. Therefore, micro-gravity experiments should be conducted for methane/air mixtures near the lean flammability limit ($\varphi \leqslant 0.65$). In Fig. 1, only results reported by Ronney and Wachman [32] and Wang et al. [26] were obtained from micro-gravity experiments. Though good agreement is achieved for the laminar flame speeds measured in micro-gravity experiments [26,32], the measured data are much lower than numerical prediction, as shown in the enlarged inset in Fig. 1a. Furthermore, Fig. 1b shows that the negative Markstein lengths reported by Wang et al. [26] were unreasonably lower than those measured by other researchers and predicted by simulation (It is noted that in Ref. [32], the stretched flame speed at $R_f = 7$ cm was considered to be the laminar flame speed. Linear extrapolation to zero stretch rate was not conducted and thus the Markstein length was not obtained by Ronney and Wachman [32].)

The reason for these discrepancies has yet to be quantitatively explained. The difference between experimental and numerical results mentioned above could be caused by the inaccuracy of the experimental measurements, the inaccuracy of the theoretical models employed in the data processing, or/and the invalidity of the kinetic mechanism. In this study, numerical simulation is conducted to help understand the deficiencies of the models used to interpret the experimental measurement. For lean CH_4/air mixtures, there are two possible sources affecting the accuracy of the measured S_u^0 and L_b. The first one is radiation, which always exits in experiments and is important for spherical flames of near-limit mixtures [33,34]. The second one is compression, which is caused by pressure increase during the flame propagation and is important for spherical flame experiments conducted in a small chamber [35]. The objective of this study is to assess the effects of radiation and compression on the flame propagation speed and the extracted laminar flame speed and Markstein length. The effects of radiation and compression were not accounted for in the interpretation of experimental measurements. In this study, they are found to be the causes for the discrepancies between measured and calculated S_u^0 and L_b of CH_4/air mixtures near the lean flammability limit.

The paper is organized as follows: in Section 2, numerical methods and specifications are presented; then, in Section 3, the radiation and compression effects on the flame propagation speed and linear extrapolation are assessed and the radiation re-absorption effects are discussed; finally, the conclusions are summarized in Section 4.

2. Numerical methods and specifications

In order to study the effects of radiation and compression on spherical flame propagation, a time-accurate and space-adaptive numerical solver for Adaptive Simulation of Unsteady Reactive Flow, A-SURF (1D), is used to carry out high-fidelity numerical simulation of outwardly propagating spherical flames. A-SURF has been successfully used and validated in a series of studies on spherical flame initiation and propagation [23,24,30,35,36].

The unsteady Navier–Stokes equations and the energy and species conservation equations for a multi-species reactive mixture in a one-dimensional spherical coordinate are solved in A-SURF [23]:

$$\frac{\partial U}{\partial t} + \frac{1}{r^2}\frac{\partial F(U)}{\partial r} = \frac{1}{r^2}\frac{\partial F_v(U)}{\partial r} + S_R \quad (1)$$

where the vectors U, $F(U)$, $F_v(U)$, and S_R are defined as

$$U = \begin{pmatrix} \rho Y_1 \\ \rho Y_2 \\ \vdots \\ \rho Y_n \\ \rho u \\ E \end{pmatrix}, \quad F(U) = \begin{pmatrix} r^2 \rho u Y_1 \\ r^2 \rho u Y_2 \\ \vdots \\ r^2 \rho u Y_n \\ r^2(\rho u^2 + P) \\ r^2(E+P)u \end{pmatrix},$$
$$F_v(U) = \begin{pmatrix} -r^2 \rho Y_1 V_1' \\ -r^2 \rho Y_2 V_2' \\ \vdots \\ -r^2 \rho Y_n V_n' \\ r^2 \tau_1 \\ r^2 q \end{pmatrix}, \quad S_R = \begin{pmatrix} \omega_1 \\ \omega_2 \\ \vdots \\ \omega_n \\ -2\tau_2/r \\ q_r \end{pmatrix} \quad (2)$$